

Electron Transfer in Organometallic Clusters. 12.¹ Regioselective Sequential Electrocatalytic Substitution of [μ -(CF₃)₂C₂]Co₂(CO)₆ by Polydentate Ligands

Robert G. Cunninghame, Lyall R. Hanton, Simon D. Jensen, Brian H. Robinson,* and Jim Simpson*

Department of Chemistry, University of Otago, P.O. Box 56, Dunedin, New Zealand

Received December 4, 1986

Selective catalytic ligation of [μ -(CF₃)₂C₂]Co₂(CO)₆ with the ligands dppm [bis(diphenylphosphino)methane], dppe [bis(diphenylphosphino)ethane], and ttas [bis(*o*-(dimethylarsino)phenyl)methylarsine] is described. Catalysis was initiated by benzophenone ketyl or a cathode, and the yields of the products are correlated with those from analogous thermal reactions. The catalytic efficiency for the stages of selective substitution was independent of the ligand, but the rate of substitution and the resultant ligand configuration does depend on the bite of the ligand. Products characterized are [μ -(CF₃)₂C₂]Co₂(CO)₅(η^1 -L-L) (L-L = dppm, ttas), [μ -(CF₃)₂C₂]Co₂(CO)₅(η^1 -L-L) (L-L = dppe), [μ -(CF₃)₂C₂]Co₂(CO)₄(η^2 -L-L) (L-L = dppm, dppe), [μ -(CF₃)₂C₂]Co₂(CO)₄(η^2 -L) (L = dppe, ttas), and [μ -(CF₃)₂C₂]Co₂(CO)₃(η^3 -ttas). [μ -(CF₃)₂C₂]Co₂(CO)₄(η^2 -dppe) crystallized in the monoclinic space group $P2_1/n$ ($Z = 4$, $a = 11.991$ (2) Å, $b = 14.335$ (4) Å, $c = 19.612$ (6) Å, $\beta = 106.86$ (2)°), and its structure was refined to $R = 0.0331$ and $R_w = 0.0340$ for 3960 reflections ($I > 3\sigma(I)$). [μ -(CF₃)₂C₂]Co₂(CO)₄(η^2 -ttas) was monoclinic, space group $P2_1/c$ ($Z = 4$, $a = 12.563$ (2) Å, $b = 15.166$ (3) Å, $c = 17.995$ (7) Å, $\beta = 114.74$ (2)°), with refinement to $R = 0.0623$ and $R_w = 0.0654$ for 1784 reflections ($I > 3\sigma(I)$). The structures of these derivatives are compared to that of the η^3 -ttas complex. The spectroscopic data show that the polydentate derivatives are stereochemically nonrigid in solution. ETC substitution is used to rapidly incorporate ¹³CO in these molecules.

Electron transfer chain (ETC) catalyzed reactions of metal carbonyl cluster substrates have been identified for a variety of monodentate and polydentate phosphine, arsine, and sulfide ligands.²⁻⁶ The attraction of ETC reactions with polydentate ligands is the ability to control the sequential substitution on one or more metal sites of the cluster, and with some substrates it is possible to synthesize partially ligated complexes which are not readily accessible by other preparative routes.^{2,4} In earlier papers we dealt with the RCCo₃(CO)₉/polydentate ligand system from both a preparative⁵ and an electrochemical point of view.⁶ In this system the electrochemical interpretation was complicated by $\bar{E}CE$ as well as $\bar{E}CE$ processes and the products with tridentate ligands were not kinetically stable. We therefore sought a system in which the derivatives are kinetically stable, where the substrate radical anion is thermodynamically and kinetically stable, and where the electrochemistry is dominated by one-electron charge transfer. The alkyne cluster (CF₃)₂C₂Co₂(CO)₆ (**1**) fulfilled these requirements,^{3,7} and herein we describe the preparative and structural study of Ph₂PCH₂PPh₂ (dppm), Ph₂P(CH₂)₂PPh₂ (dppe), and {*o*-C₆H₄[As(CH₃)₂]₂AsCH₃ (ttas) derivatives. Some preliminary results have been communicated,⁴ but there are no other reports of polydentate derivatives of **1**, although dppm and dppe derivatives of R₂C₂Co₂(CO)₆ (R = Ph, H) are well-known.^{8,9} An

electrochemical investigation of the compounds described herein is given in the following paper.¹⁰

Experimental Section

(CF₃)₂C₂Co₂(CO)₆ (**1**) was prepared from Co₂(CO)₈ and (CF₃)₂C₂ by a modification of the literature method;¹¹ (CF₃)₂C₂ and Co₂(CO)₈ were shaken together in a sealed tube for 24 h, and the resulting deep red solution was worked up as described by Dickson. ttas was prepared by the literature procedure¹² with dppm and dppe used as received (Strem). All reactions and manipulations were carried out under Ar although most products are stable in air for short periods. Solvent purification, the preparation of benzophenone ketyl (BPK), and the procedures for the bulk electrolyses have been described elsewhere.¹ NMR spectra were recorded at 90 MHz on Varian EM-390 (¹H) or JEOL spectrometers (¹³C, ¹⁹F, ³¹P) and IR spectra on Nicolet FT-IR or Perkin Elmer 225 spectrophotometers. All electrode potentials are vs. Ag/AgCl.

Reaction of 1 with dppm. (a) BPK Initiation. To an Ar-flushed 100 cm³ three-necked flask fitted with a septum cap and a gas inlet was added **1** (119 mg, 0.27 mmol), dppm (122 mg, 0.32 mmol), and THF (15 cm³). A catalytic amount of BPK (<0.1 cm³) was added via the septum cap to the vigorously stirred solution. An immediate color change from orange to red occurred as the BPK was added. The THF was removed in vacuo and the residue separated on silica gel plates (hexane); only one band other than **1** developed. Elution of this band with CH₂Cl₂ and crystallization from hexane gave **2** [μ -(CF₃)₂C₂]Co₂(CO)₅(η^1 -dppm) as orange-red prisms (211 mg, 97%): mp 116 °C (dec); IR (hexane) ν (CO) 2092 (s), 2048 (vs), 2036 (vs), 2007 (s) cm⁻¹. Anal. Calcd for C₃₄H₂₂Co₂F₆P₂O₅: C, 50.75; H, 2.76. Found: C, 51.15; H, 3.06. It is soluble in all organic solvents, but a slow conversion to **3** (see below) occurs over several days in hexane. This conversion is much

(1) Downard, A. J.; Robinson, B. H.; Simpson, J. J. *Organomet. Chem.*, in press.

(2) (a) Bezems, G. J.; Rieger, P. H.; Visco, S. *J. Chem. Soc. Chem. Commun.* **1981**, 265. (b) Bruce, M. I.; Kehoe, D. G.; Matison, J. G.; Nicholson, B. K.; Rieger, P. H.; Williams, M. L. *J. Chem. Soc. Chem. Commun.* **1982**, 442. (c) Darchen, A.; Mahe, C.; Patin, H. *J. Chem. Soc., Chem. Commun.* **1982**, 243.

(3) (a) Arewgoda, C. M.; Robinson, B. H.; Simpson, J. J. *Am. Chem. Soc.* **1983**, *105*, 1893. (b) Arewgoda, C. M.; Robinson, B. H.; Simpson, J. J. *J. Chem. Soc., Chem. Commun.* **1982**, 284.

(4) Cunninghame, R. G.; Downard, A. J.; Hanton, L. R.; Jensen, S. D.; Robinson, B. H.; Simpson, J. *Organometallics* **1984**, *3*, 180.

(5) Downard, A. J.; Robinson, B. H.; Simpson, J. *Organometallics* **1986**, *5*, 1122.

(6) Downard, A. J.; Robinson, B. H.; Simpson, J. *Organometallics* **1986**, *5*, 1132-1140.

(7) Arewgoda, C. M.; Rieger, P. H.; Robinson, B. H.; Simpson, J.; Visco, S. *J. Am. Chem. Soc.* **1982**, *104*, 5633.

(8) (a) Chia, L. S.; Cullen, W. R.; Franklin, M.; Manning, A. R. *Inorg. Chem.* **1975**, *14*, 2521. (b) Crow, J. P.; Cullen, W. R. *Inorg. Chem.* **1971**, *10*, 2165.

(9) (a) Bird, P. H.; Fraser, A. R.; Hall, D. N. *Inorg. Chem.* **1977**, *16*, 1923. (b) Bianchini, C.; Dapporto, P.; Mela, A. *J. Organomet. Chem.* **1979**, *174*, 205.

(10) Jensen, S. D.; Robinson, B. H.; Simpson, J. *Organometallics*, following paper this issue.

(11) Boston, J. L.; Sharp, D. W. A.; Wilkinson, G. *J. Chem. Soc.* **1962**, 3488.

(12) Cunninghame, R. G.; Nyholm, R. S.; Tobe, M. L. *J. Chem. Soc., Suppl. I* **1964**, 5800.

more rapid (several hours) in polar solvents like THF.

When more BPK solution (ca. 0.2 cm³) was added to the reaction solution above, or BPK (ca. 0.2 cm³) was added to a solution of **2** in THF, further reaction took place resulting in a deep red colored solution. The THF was removed in vacuo and the residue separated on silica gel plates (hexane/ether/CH₂Cl₂, 10:1:1); three major bands developed. The first band (~15%) was due to **2**. The second band (green-brown) was eluted with CH₂Cl₂ and the solvent removed in vacuo to give a small amount (~5%) of green [(μ-(CF₃)₂C₂)Co₂(CO)₄(η²-dppm) (**3'**): IR (hexane) ν(CO) 2073 (ms), 2028 (vs), 2007 (vs) cm⁻¹ (see Table V for ³¹P NMR). Attempts to obtain an analytically pure sample were unsuccessful due to its lability in solution; the predominant decomposition product is orange-red **3**.

The third band was eluted with CH₂Cl₂ and shown by the IR spectrum to be identical with **3** prepared by a thermal reaction; yield ~65%.

(b) Thermal Reaction. A hexane solution (20 cm³) containing **1** (52 mg, 0.12 mmol) and dppm and 44.6 mg, 0.12 mmol) was heated under reflux for 5 h; the reaction was monitored by TLC and IR. At no time during the reaction was there an appreciable amount of **2**. The solvent was stripped in vacuo and the residue separated on silica gel plates (hexane/ether/CH₂Cl₂, 10:1:1). Three major bands developed, the first due to **2** (~2%) and the second due to **3'** (~1%), while the third, on crystallization from hexane, yielded orange-red rhombs of [(μ-(CF₃)₂C₂)Co₂(CO)₄(η²-dppm) (**3**) (79 mg, 85%): mp 389 K; IR (hexane) ν(CO) 2059 (s), 2032 (vs), 2006 (vs) cm⁻¹. Anal. Calcd for C₃₃H₂₂Co₂F₆P₂O₄: C, 51.03; H, 2.86. Found: C, 51.25; H, 3.07. The compound is stable in all organic solvents.

(c) Bulk Electrolysis. dppm (0.11 mmol) was dissolved in CH₂Cl₂ (30 cm³) containing 0.1 mol dm⁻³ of TBAP. The solution was electrolyzed at -0.4 V vs Ag/AgCl until a steady background current was reached. **1** (0.11 mmol) was added and the electrolysis continued until the current fell near to background level, and TLC showed complete reaction of **1** (~15 min); the electrical consumption was ~0.01 F mol⁻¹. The solvent was removed and the orange residue extracted with hexane from which 84 mg of **2** crystallized (95%).

When the above procedure was repeated by using **2** instead of **1** as a substrate and a reduction potential of -0.6 V vs Ag/AgCl, a red solution was obtained with the consumption of ~0.2 F mol⁻¹. The solvent was removed, the residue extracted with hexane/ether (10:1), and the solvent removed from the extracts. This residue was separated on silica gel plates (hexane/ether, 10:1) to give **2** (~5%) and **3** (~89%) as the major products.

Reaction of 1 with dppe. **(a) BPK Initiation.** The difficulty with this reaction is that the thermal reaction of **1** with dppe is also fast in THF. To minimize this complication **1** (25.8 mg, 0.058 mmol) was dissolved in THF (5 cm³) and the dppe (24.6 mg, 0.061 mmol) and BPK (>0.1 cm³) were added together via separate necks to the solution. There was an immediate color change to deep red, and TLC analysis indicated complete reaction. The solvent was removed in vacuo and the residue separated on silica gel plates (hexane/ether, 20:1). Three bands developed. Band **1** was eluted with CH₂Cl₂, the solvent removed, and the residue crystallized from hexane to give [(μ-(CF₃)₂C₂)Co₂(CO)₅(η¹-dppe) (**4**): orange-brown rhombs (33 mg, 92%), mp 450 K decomp to **5**; IR (hexane) ν(CO) 2092 (s), 2048 (vs), 2038 (vs), 1997 (w) cm⁻¹. Anal. Calcd for C₄₄H₂₄Co₄F₁₂P₂O₁₀: C, 42.65; H, 1.95. Found: C, 43.00; H, 2.28. **4** is soluble in all organic solvents but rapidly converts to **5** and **5'** (see below), particularly in polar solvents.

Band **2** was eluted with CH₂Cl₂, the solvent removed, and the residue crystallized from hexane to give a green oil, [(μ-(CF₃)₂C₂)Co₂(CO)₄(η²-dppe) (**5'**): IR (hexane) ν(CO) 2056 (s), 2028 (vs), 2005 (vs), 1986 (w) cm⁻¹. There was an insufficient amount for NMR and analytical measurements.

Band **3** treated as above gave [(μ-(CF₃)₂C₂)Co₂(CO)₄(η²-dppe) (**5**) as red-brown prisms: mp 459 K; 2.4 mg, 5%; IR (hexane) ν(CO) 2073 (s), 2026 (vs), 2010 (vs) cm⁻¹. Anal. Calcd for C₃₄H₂₄Co₂F₆P₂O₄: C, 51.65; H, 3.06. Found: C, 51.42; H, 3.49.

When the addition of BPK/dppm was carried out at 273 K, a >98% yield of **4** was obtained with only minor amounts of **5'** and **5**.

(b) Thermal Reaction. **1** (31 mg, 0.065 mmol) and dppe (28 mg, 0.07 mmol) were heated under reflux in hexane (20 cm³) for

5 h. The solvent was removed in vacuo, and separation on silica gel (hexane/ether/CH₂Cl₂, 10:1:1) gave 3 mg of **4** (8%) and 40 mg of **5** (78%). In addition there were minor amounts of purple and red compounds with lower *R_f*.

1 (52 mg, 0.12 mmol) was dissolved in THF (15 cm³) and 46 mg of dppe (0.12 mmol) added to the stirred solution. Within 5 min the solution had turned a deep red and TLC indicated that all **1** had reacted. Workup on silica gel plates (hexane/ether, 20:1) gave 39 mg (50%) of **4** and 46 mg (48%) of **5**. In a separate experiment BPK was added after 10 min, but there was no change to the relative yields of **4** and **5**.

(c) Electrolysis. dppe (45 mg, 0.11 mmol) was dissolved in CH₂Cl₂ (30 cm³) containing 0.1 mol dm⁻³ TBAP. The solution was electrolyzed at -0.8 V vs Ag/AgCl until a steady background current was obtained. **1** (49 mg, 0.11 mmol) was added and the potential decreased to -0.4 V. The solution immediately turned red, and the background current was reached after <1 min. At this point, <0.001 F mol⁻¹ had been consumed. The solvent was removed and the residue extracted with hexane/ether (20:1) to give an orange-red solution; TLC analysis showed that only **4** was present in significant amount. The solvent was removed from the extracts, and the residue crystallized from hexane to give **4** in 98% yield. **4** (40 mg) and dppe (36 mg) dissolved in CH₂Cl₂ (25 cm³) containing 0.1 mol dm⁻³ TBAP were electrolyzed by using the procedure above at -0.6 V for 10 min. At this point 0.2 F mol⁻¹ had been consumed and workup gave **5**.

Reaction of 1 with ttas. **(a) Thermal Reaction.** ttas (49 mg, 0.11 mmol) and **1** (49 mg, 0.11 mmol) were heated under reflux in hexane (20 cm³) for 5 h with periodic monitoring of the reaction by TLC (hexane/CH₂Cl₂, 10:1). The major product during the entire course of the reaction was a purple compound with no indication of a reaction intermediate. The hexane solution was cooled to 273 K, and the black needles [(μ-(CF₃)₂C₂)Co₂(CO)₃(η³-ttas) (**8**) were removed by filtration (81 mg, 90%; mp 479 K): IR (hexane) ν(CO) 2054 (s), 2031 (vs), 1990 (vs) cm⁻¹; IR (KBr) 2024 (vs), 1979 (s), 1865 (m) cm⁻¹; mass spectrum, *m/e* (relative intensity) 816 (M⁺, 52), 788 (M - CO⁺, 100), 760 (M - 2CO⁺, 42), 732 (M - 3CO⁺, 92); another weaker sequence is seen [M - (CO)_{*n*} - F]⁺ (*n* = 0-3); metastables at *m/e* 761 (816 - 788), 733 (788 - 760), 705 (760 - 732). Anal. Calcd for C₂₄C₂₃As₃F₆O₃Co₂: C, 35.30; H, 2.82. Found: C, 36.86; H, 3.22.

A rapid reaction occurs at ambient temperatures in THF. ttas (69 mg, 0.15 mmol) was added to a stirred solution of **1** (68 mg, 0.15 mmol) in THF (20 cm³). After 3 min **1** had completely reacted as shown by TLC. The THF was stripped in vacuo and the residue separated on silica gel plates (hexane/ether/CH₂Cl₂, 20:1:1). The purple band (lowest *R_f*) was shown by IR to be **8** (yield 20%). The main product, a dark green band, was eluted with CH₂Cl₂ and crystallized from hexane/CH₂Cl₂ at 255 K to give [(μ-(CF₃)₂C₂)Co₂(CO)₄(η²-ttas) (**7**) as green black prisms (89 mg, 70%): mp 408 K; IR (hexane) ν(CO) 2075 (vs), 2029 (s), 1980 (s) cm⁻¹. Anal. Calcd for C₂₅H₂₂As₃F₆O₄Co₂: C, 35.55; H, 2.73. Found: C, 35.98; H, 2.77. This compound rapidly converts to **8** at 293 K in donor solvents such as THF (*t*_{1/2} ≈ 1 min) but more slowly in CH₂Cl₂ (*t*_{1/2} ≈ 12 min) and hexane (*t*_{1/2} ≈ 20 min). Quantitative conversion **7** → **8** can be achieved by heating **7** in hexane for ~1 h.

(b) Electrolysis. The electrolysis solution [**1** (27 mg, 0.06 mmol), CH₂Cl₂ (25 cm³), TBAP (5 × 10⁻² mol dm⁻³)] was cooled to 273 K after the solution had been electrolyzed at -0.6 V at 293 K until a steady background current had been obtained. The potential was set to -0.4 V and ttas (62 mg, 0.06 mmol) added with vigorous stirring by the gas flow. There was an immediate change to an orange color, and TLC showed that all of **1** had been consumed; the charge consumption was <0.001 F mol⁻¹. The CH₂Cl₂ was removed at 273 K and the yellow residue extracted with ice-cold hexane; removal of the hexane at 273 K gave a yellow-orange solid [(μ-(CF₃)₂C₂)Co₂(CO)₅(η¹-ttas) (**6**): IR (hexane) ν(CO) 2093 (s), 2049 (vs), 2037 (vs), 2002 (m) cm⁻¹. All attempts to crystallize this compound were unsuccessful because of the extremely rapid conversion to **7** even in the solid phase.

If the above procedure is carried out at 293 K, or if the initial potential is ~-0.6 V, the only product is the green-black complex **7** in 100% yield; efficiency ~0.01 F mol⁻¹.

Complex **8** can be produced from **6** or **7** by electrolyzing at -0.8 V in CH₂Cl₂/TBAP for several minutes until a TLC in hexane

shows only a purple band. Air is admitted to the system, and workup as above for the thermal preparation gives 8 (~80% yield); charge consumption ~1 F mol⁻¹. This is not the recommended method for the formation of 8.

(c) **BPK Initiation.** 1 (48 mg, 0.11 mmol) was dissolved in THF (10 cm³) at 263 K; ttas (48 mg, 0.11 mmol) was added as a solid simultaneously with BPK (~0.1 cm³). The timing is essential because of the rapid thermal reaction. A dark green-brown color developed in the solution as the purple color of BPK faded over ~2 min. The THF was stripped in vacuo, and separation as for the thermal reaction gave 7 (90%) with a trace of 8.

Reaction of [μ -Ph₂C₂]Co₂(CO)₆ with ttas. BPK (~0.1 cm³) was added to a THF (15 cm³) solution containing Ph₂C₂Co₂(CO)₆ (55 mg, 0.12 mmol) and ttas (56 mg, 0.12 mmol). There was no observable color change, and the solution was stirred for 70 min. Trace amounts of three green products were separated on silica gel plates (hexane/ether, 10:1). Only two were characterized by IR spectra (in order of R_f): IR (hexane): A, ν (CO) 2064 (vs), 2015 (vs), 2008 (s), 1968 (m) cm⁻¹; B, ν (CO) 2045 (vs), 1997 (s), 1966 (m), 1946 (m) cm⁻¹. Both products were unstable in organic solvents.

¹³CO Substitution by BPK-Initiated ETC Reactions. 1 (0.127 g) was dissolved in THF (20 cm³) and the flask with a septum-capped neck and magnetic stirring bar attached to a vacuum line containing the ¹³CO reservoir bulb. After a number of freeze-thaw cycles under vacuum ¹³CO (99.9%) was introduced to the evacuated flask at 77 K. The solution was brought to ambient temperature and a catalytic amount (<0.1 cm³) of BPK added through the septum. The solution immediately turned a deeper red color, and the solution was stirred until the original orange color had returned (~2 h, time does vary from run to run). The ¹³CO was removed and the solution evaporated to dryness in vacuo at 273 K. Sublimation gave 0.110 g of 1. Mass spectral analysis showed that the degree of substitution was ~12%. A higher degree of substitution (25%) was achieved by repeating the process but with use of ~0.2 cm³ of BPK; the yield was much lower, however, and undoubtedly the percent substitution can be increased further by repeating the initial procedure several times on the one sample with a sacrifice of yield. A control run was carried out in CH₂Cl₂ without BPK, but there was no evidence for ¹³CO incorporation after 4–8 h.

Crystal Structure Determination of 5. Crystals of 5, prepared as described above, were grown from hexane solutions, and an orange-red block was selected for data collection. Precession photography, using Cu K α radiation, indicated a monoclinic system, identified as the space group P2₁/n [a nonstandard orientation of P2₁/C (No. 14)]¹³ from the systematic absences $h0l$ for $h + l = 2n + 1$ and $0k0$ for $k = 2n + 1$. Data were collected at 133 \pm 1 K on a Nicolet P3, four-circle, fully automated diffractometer. The cell dimensions and orientation matrices were calculated from 15 accurately centred reflections. Relevant details of the crystal, data collection, solution, and refinement are summarized in Table I. Data were processed by using programs from the SHELXTL package.¹⁴

The structure was solved by using the EES direct methods routine in program SHELX.¹⁵ The highest ranked of the resulting E maps revealed the location of the two cobalt and two phosphorus atoms. The remaining non-hydrogen atoms were found in a single difference Fourier synthesis following least-squares refinement¹⁶ of these parameters. Refinement with all non-hydrogen atoms assigned isotropic thermal parameters converged with $R = 0.069$. Numerical absorption corrections were applied,¹⁵ hydrogen atoms were included in calculated positions ($d_{C-H} = 1.08$ Å), and all non-hydrogen atoms were assigned anisotropic thermal parameters. The structure was then refined in alternating blocked matrix cycles, and a weighting scheme was introduced. The function minimized was $\sum w(|F_o| - |F_c|)^2$ for the 3960 observed reflections. Refinement of this model converged with $R = 0.0331$ and $R_w =$

Table I. Crystal Data, Data Collections, and Refinements of 5 and 7

	5	7
Crystal Data		
cryst system	monoclinic	monoclinic
space group	P2 ₁ /n	P2 ₁ /c
<i>a</i> , Å	11.991 (2)	12.563 (2)
<i>b</i> , Å	14.335 (4)	15.166 (3)
<i>c</i> , Å	19.612 (6)	17.995 (7)
β , deg	106.86 (2)	114.74 (2)
<i>V</i> , Å ³	3226 (1)	3113.91
formula	C ₂₄ H ₂₄ O ₄ F ₆ P ₂ Co ₂	C ₂₃ H ₂₃ O ₄ F ₆ As ₃ Co ₂
fw	790.4	844.1
D_{calcd} , g cm ⁻³	1.63	1.87
D_{measd} , g cm ⁻³	1.66 (floatation)	
<i>Z</i>	4	4
$F(000)$	1592	1648
cryst size, mm	0.56 \times 0.44 \times 0.28	0.15 \times 0.20 \times 0.90
μ , cm ⁻¹	12.5 (Mo K α)	121.7 (Cu K α)
Data Collections and Refinements		
diffractometer	Nicolet P3	Hilger and Watts
radiatn, Å	Mo K α ($\lambda =$ 0.71069) (graphite mono- chromator)	Cu K α ($\lambda = 1.5148$) (nickel filter)
scan type	θ - 2θ	θ - 2θ
data limits	$0 < 2\theta < 50^\circ$	$1 < 2\theta < 50^\circ$
reflections measd	$\pm h, k, l$	$h, k, \pm l$
cryst decay	<2% ^a	<5% ^b
total obsd data	5053 ($R_{\text{int}} = 0.0118$)	3237 ($R_{\text{int}} = 0.0389$)
unique data	3960 ($I < 3\sigma(I)$)	1784 ($I > 3\sigma(I)$)
absorption correctn	numerical ^c	numerical ^d
maximum	0.8395 (transmission)	12.663 (correction)
minimum	0.7084 (transmission)	3.115 (correction)
no. of variables	219 (209) ^e	378
R ($\sum F_o - F_c / \sum F_o $)	0.0331	0.0623
R_w ($\sum w^{1/2} F_o - F_c / \sum w^{1/2} F_o $)	0.0340	0.0654
w	[1.5080/ $(\sigma^2(F) +$ 0.000198 $F^2)$]	[1.000/ $\sigma^2(F) +$ 0.00149 $F^2)$]

^a Standard reflections (800), (060), and (006) measured after every 100 reflections. ^b Standard reflections (0,-14,0), (114), and (600) measured after every 100 reflections. ^c See ref 14. ^d See ref 18. ^e In each of the blocked matrix refinements.

0.0340. The highest peak in the final difference Fourier synthesis was ~0.38 e Å⁻³.

Crystal Structure Determination of 7. Crystals of 7 were grown from CH₂Cl₂/hexane solution as described above, and a green/black needle was selected and used for data collection. Precession and Weissenberg photography (Cu K α radiation) indicated a monoclinic system, and the systematic absences $h0l$ ($l = 2n + 1$) and $0k0$ ($k = 2n + 1$) were consistent with the space group P2₁/c (No. 14).¹³ Diffraction data were collected at 293 \pm 1 K on a Hilger and Watts, four-circle computer controlled diffractometer. The unit cell dimensions and orientation matrices were calculated from 12 accurately centered reflections. Details of the crystal, data collection, and structure refinement are summarized in Table I. The data were processed by using the program HILGOUT¹⁶ and analytical absorption corrections applied with the program ABSORB.¹⁷

The structure was solved by using the direct methods program EES from the SHELX package.¹⁵ The highest ranked E map revealed the location of the two cobalt and three arsenic atoms together with the intervening carbon atoms of the triarsenic skeleton. The remaining non-hydrogen atoms were located in successive difference Fourier syntheses and least-squares refinements. Hydrogen atoms were introduced in calculated positions ($d_{C-H} = 1.08$ Å) and the non-hydrogen atoms assigned

(13) *International Tables for X-ray Crystallography*, 3rd ed.; Kynoch: Birmingham, England, 1969; Vol. 1.

(14) Sheldrick, G. M. SHELXTL, An integrated system for solving refining and displaying crystal structures from diffraction data; University of Göttingen: Göttingen, Federal Republic of Germany, 1980; p 15.

(15) Sheldrick, G. M. SHELX, Program for Crystal Structure Determination; University of Cambridge: Cambridge, England, 1975.

(16) The data processing program HILGOUT is based on the programs DRED (J. F. Blount) and PICKOUT (R. J. Doedens).

(17) Program ABSORB, a major modification of AGNOST (L. Templeton and D. Templeton).

Table II. Final Positional and Equivalent Thermal Parameters for 5

atom	<i>x/a</i>	<i>y/b</i>	<i>z/c</i>	<i>U_{eq}</i> , Å ²
Co(1)	-0.7088 (1)	-0.3311 (1)	0.1150 (1)	0.013
Co(2)	-0.7290 (1)	-0.4098 (1)	-0.0018 (1)	0.015
C(1)	-0.7706 (3)	-0.1992 (2)	-0.0278 (2)	0.023
C(2)	-0.7601 (3)	-0.2796 (2)	0.0198 (2)	0.014
C(3)	-0.8408 (3)	-0.3380 (2)	0.0329 (2)	0.015
C(4)	-0.9685 (3)	-0.3433 (2)	0.0114 (2)	0.023
F(1)	-0.6797 (2)	-0.1886 (2)	-0.0547 (1)	0.040
F(2)	-0.7818 (3)	-0.1176 (1)	0.0022 (1)	0.055
F(3)	-0.8644 (2)	-0.2055 (1)	-0.0865 (1)	0.038
F(4)	-1.0098 (2)	-0.4128 (1)	0.0433 (1)	0.032
F(5)	-1.0160 (2)	-0.2636 (1)	0.0286 (1)	0.036
F(6)	-1.0172 (2)	-0.3545 (2)	-0.0590 (1)	0.035
C(11)	-0.7239 (5)	-0.4315 (2)	0.1649 (2)	0.019
O(11)	-0.7382 (2)	-0.4985 (2)	0.1935 (1)	0.035
C(21)	-0.5854 (3)	-0.3963 (2)	-0.0140 (2)	0.019
O(21)	-0.4979 (2)	-0.3840 (2)	-0.0237 (1)	0.031
C(22)	-0.7357 (3)	-0.5275 (2)	0.0301 (2)	0.020
O(22)	-0.7413 (2)	-0.6017 (2)	0.0503 (1)	0.026
C(23)	-0.8139 (3)	-0.4286 (2)	-0.0929 (2)	0.023
O(23)	-0.8684 (2)	-0.4434 (2)	-0.1498 (1)	0.039
P(1)	-0.7517 (1)	-0.2338 (1)	0.1912 (0)	0.015
P(2)	-0.5195 (1)	-0.3013 (1)	0.1654 (0)	0.016
C(31)	-0.6147 (3)	-0.2136 (2)	0.2629 (2)	0.020
C(32)	-0.5096 (3)	-0.2101 (2)	0.2336 (2)	0.021
C(41)	-0.8506 (3)	-0.2722 (2)	0.2415 (2)	0.016
C(42)	-0.9338 (3)	-0.3421 (2)	0.2155 (2)	0.023
C(43)	-1.0090 (3)	-0.3684 (3)	0.2547 (2)	0.028
C(44)	-1.0002 (3)	-0.3278 (2)	0.3199 (2)	0.027
C(45)	-0.9175 (3)	-0.2590 (2)	0.3464 (2)	0.024
C(46)	-0.8435 (3)	-0.2309 (2)	0.3070 (2)	0.022
C(51)	-0.8095 (3)	-0.1185 (2)	0.1601 (2)	0.018
C(52)	-0.9301 (3)	-0.1023 (2)	0.1407 (2)	0.027
C(53)	-0.9740 (3)	-0.0167 (3)	0.1132 (2)	0.037
C(54)	-0.9010 (3)	0.0542 (3)	0.1052 (2)	0.034
C(55)	-0.7816 (3)	0.0389 (2)	0.1251 (2)	0.030
C(56)	-0.7366 (3)	-0.0464 (2)	0.1520 (2)	0.022
C(61)	-0.4247 (3)	-0.2505 (2)	0.1164 (2)	0.021
C(62)	-0.4607 (3)	-0.1687 (2)	0.0773 (2)	0.030
C(63)	-0.3894 (4)	-0.1274 (3)	0.0417 (2)	0.041
C(64)	-0.2826 (4)	-0.1658 (3)	0.0436 (2)	0.043
C(65)	-0.2467 (3)	-0.2469 (3)	0.0824 (2)	0.037
C(66)	-0.3170 (3)	-0.2895 (3)	0.1185 (2)	0.027
C(71)	-0.4327 (3)	-0.4003 (2)	0.2112 (2)	0.018
C(72)	-0.3405 (3)	-0.3903 (2)	0.2739 (2)	0.025
C(73)	-0.2752 (3)	-0.4676 (3)	0.3053 (2)	0.028
C(74)	-0.2989 (3)	-0.5548 (2)	0.2746 (2)	0.030
C(75)	-0.3886 (3)	0.5651 (2)	0.2119 (2)	0.031
C(76)	-0.4551 (3)	-0.4886 (2)	0.1808 (2)	0.026

anisotropic temperature factors. A weighting scheme based on counting statistics was introduced, and refinement converged with $R = 0.0623$ and $R_w = 0.0654$ for the 1784 observed reflections. In a final difference Fourier map, the largest residual peak appeared with a height of $0.78 \text{ e } \text{Å}^{-3}$. In both determinations, neutral atom scattering factors for the cobalt and arsenic atoms were taken from Cromer and Mann,¹⁸ with corrections for anomalous dispersion from Cromer and Liberman.¹⁹ Final positional and equivalent thermal parameters are listed for 5 in Table II and for 7 in Table III.

Results and Discussion

Substitution reactions of $[\mu\text{-(CF}_3)_2\text{C}_2]\text{Co}_2(\text{CO})_6$ (1) with the Lewis bases containing two (dppm, dppe) or three (ttas) accessible donor atoms were initiated by catalytic (electrochemical, chemical) or thermal methods. The extent of substitution and the stereochemistry of the products were a function of the method of initiation, solvent, temperature, and ligand. Scheme I summarizes the reactions with dppm and dppe; a scheme for ttas is given in ref 4.

(18) Cromer, D. T.; Mann, J. B. *Acta Crystallogr., Sect. A: Cryst. Phys., Diffraction, Theor. Gen. Crystallogr.* 1968, A24, 321.

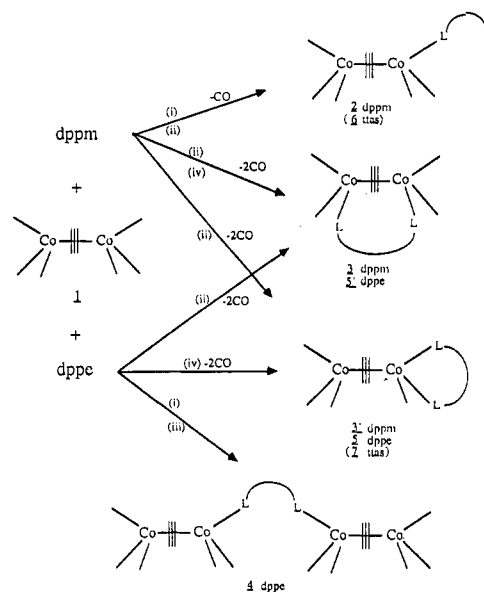
(19) Cromer, D. T.; Liberman, D. *J. Chem. Phys.* 1970, 53, 1891.

Table III. Final Positional and Equivalent Thermal Parameters for 7

atom	<i>x/a</i>	<i>y/b</i>	<i>z/c</i>	<i>U_{eq}</i> , Å ²
Co(1)	0.4028 (2)	0.7847 (2)	0.0561 (2)	0.051
Co(2)	0.5127 (3)	0.7080 (2)	-0.0109 (2)	0.068
As(1)	0.3889 (2)	0.8716 (1)	0.1560 (1)	0.062
As(2)	0.2613 (2)	0.6937 (1)	0.0690 (1)	0.057
As(3)	0.0426 (2)	0.8484 (2)	-0.0295 (2)	0.092
C(31)	0.517 (2)	0.883 (2)	0.263 (1)	0.099
C(32)	0.345 (2)	0.994 (1)	0.130 (1)	0.092
C(33)	0.308 (2)	0.579 (1)	0.121 (1)	0.082
C(34)	-0.094 (2)	0.853 (2)	-0.004 (2)	0.140
C(35)	-0.026 (2)	0.904 (2)	-0.136 (2)	0.118
C(41)	0.262 (2)	0.828 (1)	0.182 (1)	0.065
C(42)	0.208 (2)	0.753 (1)	0.147 (1)	0.067
C(43)	0.119 (2)	0.716 (2)	0.162 (2)	0.099
C(44)	0.086 (2)	0.754 (2)	0.218 (2)	0.118
C(45)	0.139 (2)	0.828 (2)	0.255 (1)	0.101
C(46)	0.236 (2)	0.868 (1)	0.242 (1)	0.108
C(51)	0.115 (2)	0.664 (1)	-0.024 (1)	0.071
C(52)	0.032 (2)	0.724 (2)	-0.066 (1)	0.090
C(53)	-0.071 (3)	0.699 (2)	-0.131 (2)	0.105
C(54)	-0.088 (2)	0.614 (2)	-0.159 (2)	0.117
C(55)	-0.006 (2)	0.553 (2)	-0.0120 (2)	0.105
C(56)	0.102 (2)	0.574 (2)	-0.049 (1)	0.088
C(21)	0.423 (2)	0.610 (2)	-0.038 (1)	0.074
O(21)	0.366 (1)	0.550 (1)	-0.055 (1)	0.103
C(22)	0.650 (2)	0.668 (1)	-0.008 (1)	0.091
O(22)	0.735 (2)	0.637 (1)	-0.001 (1)	0.135
C(23)	0.471 (2)	0.774 (1)	-0.100 (2)	0.088
O(23)	0.445 (2)	0.819 (1)	-0.157 (1)	0.119
C(11)	0.315 (2)	0.849 (1)	-0.027 (1)	0.077
O(11)	0.269 (1)	0.893 (1)	-0.083 (1)	0.102
C(1)	0.625 (2)	0.671 (2)	0.176 (2)	0.090
C(2)	0.547 (2)	0.725 (1)	0.104 (1)	0.068
C(3)	0.561 (1)	0.800 (1)	0.070 (1)	0.061
C(4)	0.644 (2)	0.872 (2)	0.090 (2)	0.084
F(11)	0.588 (1)	0.5876 (9)	0.1738 (8)	0.115
F(12)	0.636 (1)	0.7001 (9)	0.2450 (9)	0.126
F(13)	0.732 (1)	0.660 (1)	0.1812 (9)	0.144
F(41)	0.656 (1)	0.9220 (8)	0.1518 (9)	0.119
F(42)	0.627 (2)	0.924 (1)	0.029 (1)	0.195
F(43)	0.751 (2)	0.842 (1)	0.110 (1)	0.174

^a Equivalent isotropic *U* defined as one-third of the trace of the orthogonalized U_{ij} tensor.

Scheme I^a



^a (i) BPK, $<0.1 \text{ cm}^3$, THF; (ii) BPK excess, THF, 293 K; (iii) electrolysis, -0.4 V , CH_2Cl_2 ; (iv) electrolysis, -0.6 V , CH_2Cl_2 . \equiv corresponds to the acetylene ligand $(\text{CF}_3)_2\text{C}_2$.

To simplify the discussion we can first consider the possible regioisomers in general terms. For the partially

ligated compounds there are other alternatives than those depicted in Scheme I, but the coordination shown is based on the established preference of monodentate ligands for this mode of coordination in μ -alkyne cobalt complexes.^{8a,20,21} The only exceptions to this rule are the MeCN derivatives^{3a} where the small size of this ligand facilitates pseudoequatorial coordination. A pseudoequatorial ligand configuration is also adopted in $[\mu\text{-Ph}_2\text{C}_2\text{Co}_2(\text{CO})_4(\mu\text{-}\eta^2\text{-dppm})]$ ⁹ where the ligand spans the Co-Co bond; this configuration is followed in Scheme I for the $\mu\text{-}\eta^2$ derivatives. The pseudoaxial-equatorial configuration depicted for the η^2 compounds was established from the x-ray analysis described below and is similar to that found in $[\mu\text{-Ph}_2\text{C}_2\text{Co}_2(\text{CO})_4(\text{triphos})]$.^{9b}

Synthesis. dppm. A quantitative yield of the red complex $[\mu\text{-(CF}_3)_2\text{C}_2\text{Co}_2(\text{CO})_5(\eta^1\text{-dppm})]$ (2) was obtained within 1 min by the addition of a catalytic amount of BPK to a 1/dppm/THF solution at 288 K. This complex is also obtained in >90% yield by the controlled potential electrolysis of 1/dppm/CH₂Cl₂ solutions at -0.40 V vs. Ag/AgCl at 288 K with an efficiency of <0.01 F mol⁻¹.

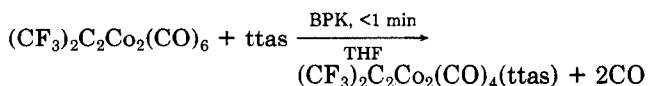
In contrast, the thermal reaction in hexane gave an orange complex, $[\mu\text{-(CF}_3)_2\text{C}_2\text{Co}_2(\text{CO})_4(\mu\text{-}\eta^2\text{-dppm})]$ (3). This complex is also produced, together with green $[\mu\text{-(CF}_3)_2\text{C}_2\text{Co}_2(\text{CO})_4(\eta^2\text{-dppm})]$ (3') if the BPK-initiated reactions in THF are left for several minutes before workup or if excess BPK is added. Greater selectivity is achieved by the controlled electrolysis of 1 with dppm in CH₂Cl₂ at -0.65 V vs. Ag/AgCl; an 89% yield of 3 was obtained with an efficiency of 0.2 F mol⁻¹.

Ring closure 2 \rightarrow 3 (3') is rapid in THF in sunlight ($t_{1/2} \approx 5$ min at 298 K) but negligible in hexane or CH₂Cl₂. Even at 273 K, 3' rapidly converts to 3 in all solvents.

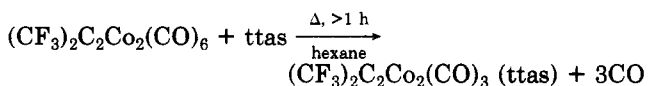
dppe. BPK initiation of the reaction of 1 with dppe in THF at 293 K gave near quantitative yields of the linked complex $\{[\mu\text{-(CF}_3)_2\text{C}_2\text{Co}_2(\text{CO})_5]_2(\mu\text{-}\eta^1\text{-dppe})\}$ (4). Cathode-induced reaction at -0.4 V in CH₂Cl₂ gave a quantitative yield of 4 with a catalytic efficiency of <0.001 F mol⁻¹.

The thermal reaction between 1 and dppe is also fast in THF at 293 K, the products being 4 and $[\mu\text{-(CF}_3)_2\text{C}_2\text{Co}_2(\text{CO})_4(\eta^2\text{-dppe})]$ (5) with trace amounts of $[\mu\text{-(CF}_3)_2\text{C}_2\text{Co}_2(\text{CO})_4(\mu\text{-}\eta^2\text{-dppe})]$ (5'). Better yields of 5 were obtained by reaction in refluxing hexane. Alternatively, a selective conversion of 1 to 5 is achieved by a cathode-induced reaction at -0.65 V in CH₂Cl₂ with a catalytic efficiency of 0.1 F mol⁻¹. The rearrangement of 4 to 5 is fast at ambient temperature in polar solvents such as THF but slow in hexane and CH₂Cl₂.

ttas. The initial product of the BPK-catalyzed reaction of 1 with ttas at ambient temperature in >95% yield is the green, labile derivative $[\mu\text{-(CF}_3)_2\text{C}_2\text{Co}_2(\text{CO})_4(\eta^2\text{-ttas})]$ (7).



7 can be converted to the purple, thermally stable, fully ligated product $[\mu\text{-(CF}_3)_2\text{C}_2\text{Co}_2(\text{CO})_3(\eta^3\text{-ttas})]$ (8); 8 is the only product in the thermal reaction of 1 with ttas in hexane.



However, the "thermal" reaction between 1 and ttas in

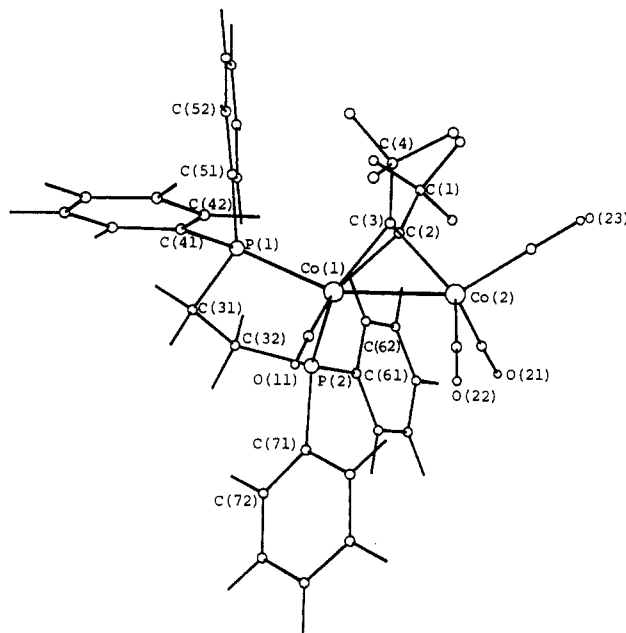
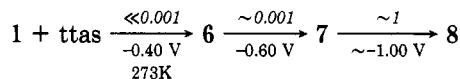


Figure 1. Structure of 5 showing the atom numbering scheme.

THF is rapid at room temperature to give a high yield of 7 with traces of the precursor complex $[\mu\text{-(CF}_3)_2\text{C}_2\text{Co}_2(\text{CO})_5(\eta^1\text{-ttas})]$ (6); with longer reaction times the initially formed 7 is converted to 8.

Sequential ligation was achieved by controlled potential electrolysis;⁴ the efficiencies (F mol⁻¹) are *italicized* for each step. 6 is very labile—even at 273 K, it converts to 7, with a half-life of ~ 2 min in hexane.



It was of interest to study the ETC reaction of ttas with $\text{Ph}_2\text{C}_2\text{Co}_2(\text{CO})_6$ for purposes of a comparison between 1⁻ and a radical anion which is relatively unstable.^{7,22} However, the extent of reaction was very low, and only two products could be isolated and characterized by IR. Comparison of these spectra with those of 6–8 suggests that the products are analogous to 6 and 7.

Structures of the Chelated Derivatives 5 and 7. The close similarity between 5 and 7 permits a joint discussion of their molecular structures. Selected interatomic distances and angles for both molecules are listed in parallel columns in Table IV together with the comparable parameters for 8.⁴ The structures of 5 and 7 consist of discrete molecular units with the closest intermolecular contacts not involving hydrogen atoms being 3.02 Å between atoms O(23) and F(1) for 5 and 3.05 Å between atoms O(11) and F(5) for 7. Figure 1 shows a general view of the structure of 5 and defines the atom numbering scheme with a comparable presentation of 7 in Figure 2.

Molecules of 5 and 7 consist of a (μ -alkyne)dicobalt core, $[\mu\text{-(CF}_3)_2\text{C}_2\text{Co}_2]$, with classical "sawhorse" arrangements²³ of the non-acetylene ligands with respect to the two cobalt atoms. In 5 the two phosphorus atoms of the dppe ligand chelate to a single cobalt atom, while the potentially tridentate ttas ligand in 7 chelates similarly via only two of its arsenic donor atoms.

The coordination geometry about each cobalt atom in both compounds can be described as considerably distorted octahedral. The two octahedra share a common face defined by the central atoms C(2) and C(3) of the alkyne

(20) Bonnet, J.-J.; Mathieu, R. *Inorg. Chem.* 1978, 17, 1973.

(21) Dickson, R. S.; Fraser, P. J. *Adv. Organomet. Chem.* 1974, 12, 323.

(22) Dickson, R. S.; Peake, B. M.; Rieger, P. H.; Robinson, B. H.; Simpson, J. J. *Organomet. Chem.* 1979, 172, C63.

(23) Thorn, D. L.; Hoffman, R. *Inorg. Chem.* 1978, 17, 126.

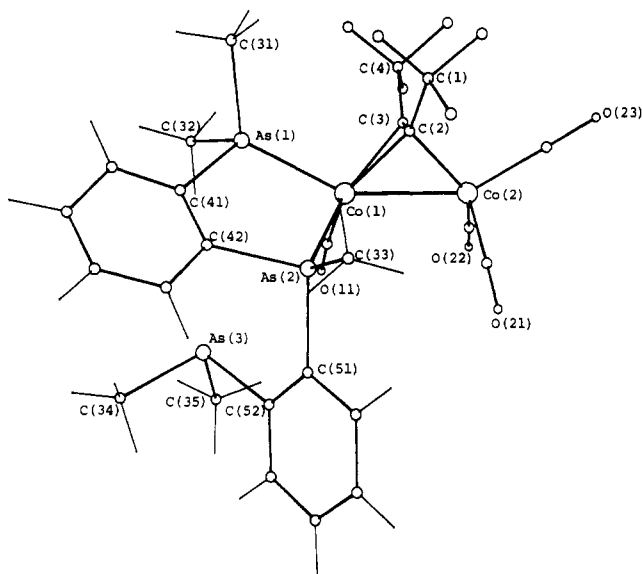


Figure 2. Structure of 7 showing the atom numbering scheme.

ligand and the "bent" Co–Co bond. In 3 the phosphorus atoms of dppe occupy the pseudoaxial, P(1), and one of the pseudoequatorial sites, P(2), on Co(1), a solid-state geometry very similar to that of $[\mu\text{-Ph}_2\text{C}_2]\text{Co}_2(\text{CO})_4$ (triphos).^{9b} A comparable arrangement is found for 7; one terminal As(1)Me₂ group coordinates to a pseudoaxial position with the central As(2)Me group pseudoequatorial. The third donor atom of the ttas ligand, As(3), is uncoordinated and is located some 4.3 Å below As(1) well away from any possible coordinative interaction with the rest of the molecule.

In both molecules the geometry about Co(2) is essentially unaffected by coordination to the adjacent cobalt atom with the carbonyl coordination mirroring that observed in the precursor $[\mu\text{-R}_2\text{C}_2]\text{Co}_2(\text{CO})_6$ molecules.^{3,24} The two equatorial carbonyl groups and the central carbon atoms of the acetylene ligands constitute the equatorial planes of octahedra with the Co(1) atoms displaced toward the axial Co ligands by 0.664 (2) Å in 5 and 0.335 (4) Å in 7. The pseudoequatorial substituents on adjacent cobalt atoms remain in an approximately eclipsed conformation following the η^2 -coordination of the ligands. This is in sharp contrast to the structure of 8 where all three arsenic donor atoms chelate to a single cobalt atom.⁴ Following η^3 -coordination the "sawhorse" geometry of the Co₂L₆ unit was destroyed with a quasi-prismatic arrangement of carbonyl ligands around Co(2). Furthermore the asymmetric electron density distribution in 8 led to the adoption of a semibridging carbonyl configuration, a phenomenon that is entirely absent in the structures reported here. Clearly the additional electron density that accrues to the Co₂C₂ unit on η^2 -coordination is insufficient to provoke the molecular rearrangement observed in 8.

The Co(1)–Co(2) bond length in 7 (2.471 (4) Å) is unexceptional whereas the corresponding vector in 5 (2.502 (1) Å) is significantly longer than those observed in a variety of other (μ -alkyne)dicobalt complexes.^{4,9,20,24} Lengthening of the Co–Co bond to >2.50 Å has been observed in $[\mu\text{-Ph}_2\text{C}_2]\text{Co}_2(\text{CO})_4$ (triphos) where it was ascribed to steric interactions^{9b} and in the bis(diphenylarsino)methane complex $[\mu\text{-Ph}_2\text{C}_2]\text{Co}_2(\text{CO})_2$ (dam)₂, where

the extension was attributed to the electronic consequences of the (μ - η) diarsine ligands occupying pseudoequatorial sites on the cobalt atoms.^{9a} In the case of 5, we favor an explanation based on steric effects; in particular, the much greater steric requirements of the Ph₂P moieties of the dppe (and triphos) ligands in comparison to the ttas complexes 7 and 8, where the donor atoms carry methyl substituents. The effect of minimizing the steric requirements of ligands to the Co₂C₂ cluster unit on the metal-metal separation is also well displayed in the molecule $[\mu\text{-H}_2\text{C}_2]\text{Co}_2(\text{CO})_4(\text{PMe}_3)_2$ where the Co–Co bond distance is unremarkable at 2.464 (1) Å despite the coordination of two phosphine ligands in pseudoaxial positions on the Co₂C₂ core.

Coordination of the (CF₃)₂C₂ ligand to the Co₂(CO)₄-(L-L) moieties generates a tetrahedral unit with approximate C₂ symmetry typical of the class of "perpendicular" acetylene complexes.²⁵ The C(2)–C(3) bond lengths are 1.360 (5) Å for 5 and 1.34 (2) Å for 7, with "bend back" angles²⁶ of the CF₃ substituents on the cis-bent acetylenes in the range 42–48°. The variation in these angles and the observation that the CF₃ substituents are twisted out of the plane of the acetylene (dihedral angles C(1)–C(2)–C(3)–C(4) = 5.9° for 5 and 12.9° for 7) indicate that the final geometry of the acetylene ligands is determined by the need to minimize nonbonding interactions between the CF₃ groups and the dppe and ttas ligands. Further evidence for the importance of the alkyne/ligand interactions in determining the overall structure derives from the observed widening of the E(1)–Co(1)–Co(2) (E = P, As) angles in comparison to those involving the less sterically demanding carbonyl pseudoaxial substituents (P(1)–Co(1)–Co(2) = 157.4 (1)° and Co(1)–Co(2)–C(22) = 148.4 (1)° for 5; As(1)–Co(1)–Co(2) = 153.4 (1)° and Co(1)–Co(2)–C(22) = 150.1 (7)° for 7) and from the unusual extension of the Co–Co bond in 5 (vide supra).

The dppe ligand chelates to the cluster with cobalt-phosphorus distances of Co(1)–P(1) = 2.211 (1) Å and Co(1)–P(2) = 2.239 (1) Å. The five-membered Co(1)–P(1)–C(31)–C(32)–P(2) ring has the usual puckered (λ or δ) geometry with the C(31) and C(32) atoms, 0.466 (3) and 0.126 (3) Å, respectively, on opposite sides of the P(1)–Co(1)–P(2) mean plane. P–C bond lengths and angles around the phosphorus atoms are all normal.

Conformations of the Arsenic Ligand. Within the ligand itself there is no significant difference between the bond lengths and angles about the coordinated arsenic atoms, As(1) and As(2), in 7 and the corresponding parameters in 8. Bond angles (mean 98°) about the uncoordinated arsenic atom, As(3), in 7 are less than those (mean 102°) about the two coordinated arsenic atoms, As(1) and As(2). However, this merely reflects the change from three- to four-coordination about arsenic, and the values found for the compounds discussed here lie within the ranges observed for a variety of ttas compounds.²⁷ The slight shortening of the C(41)–C(42) bond compared to the C(51)–C(52) bond in 7, although barely significant in this case, is consistent with the difference observed for η^2 -coordination of ttas in Ni(ttas)₂(ClO₄)₂.²⁷ Overall, the conformations of the ttas ligand in 7 and 8 are typical of those in a variety of other compounds.^{27,28}

In both 7 and 8 there is a slight variation in the Co–As bond lengths, but we do not consider this to be of major

(24) (a) Sly, W. G. *J. Am. Chem. Soc.* **1959**, *81*, 18. Bailey, N.; Mason, R. *J. Chem. Soc. A* **1968**, 1293. Penfold, B. R. Dellacca, R. *J. Inorg. Chem.* **1971**, *10*, 1269. (b) Cotton, F. A.; Jamerson, J. D.; Stults, B. R. *J. Am. Chem. Soc.* **1976**, *98*, 1774. (c) Gregson, D.; Howard, J. A. K. *Acta Crystallogr.*, **1983**, *C39*, 1024.

(25) Hoffman, D. M.; Hoffmann, R.; Fisel, C. R. *J. Am. Chem. Soc.* **1982**, *104*, 3858.

(26) Farrar, D. H.; Payne, N. C. *Inorg. Chem.* **1981**, *20*, 821.

(27) Cunningham, R. G.; Hanton, L. R., structures to be published.

(28) Blundell, T. L.; Powell, H. M. *J. Chem. Soc. A* **1971**, 1685.

Table IV. Selected Bond Lengths and Angles for 5, 7, and 8

5		7		8 ^a	
Bond Lengths (Å)					
Co(1)-Co(2)	2.502 (1)	Co(1)-Co(2)	2.471 (4)	Co(1)-Co(2)	2.454 (3)
Co(1)-C(2)	1.936 (3)	Co(1)-C(2)	1.88 (2)	Co(1)-C(2)	1.92 (2)
Co(1)-C(3)	1.906 (3)	Co(1)-C(3)	1.92 (2)	Co(1)-C(3)	1.93 (2)
Co(2)-C(2)	1.974 (3)	Co(2)-C(2)	1.94 (2)	Co(2)-C(2)	1.94 (2)
Co(2)-C(3)	1.962 (3)	Co(2)-C(3)	1.92 (2)	Co(2)-C(3)	1.92 (2)
C(1)-C(2)	1.466 (5)	C(1)-C(2)	1.51 (3)	C(1)-C(2)	1.45 (2)
C(2)-C(3)	1.360 (5)	C(2)-C(3)	1.34 (2)	C(2)-C(3)	1.34 (2)
C(3)-C(4)	1.467 (4)	C(3)-C(4)	1.45 (3)	C(3)-C(4)	1.50 (2)
Co(1)-P(1)	2.211 (1)	Co(1)-As(1)	2.294 (3)	Co(1)-As(1)	2.311 (3)
Co(1)-P(2)	2.239 (1)	Co(1)-As(2)	2.337 (3)	Co(1)-As(2)	2.280 (2)
				Co(1)-As(3)	2.316 (3)
P(1)-C(31)	1.850 (3)	As(1)-C(41)	1.97 (2)	As(1)-C(41)	1.94 (2)
P(2)-C(32)	1.850 (4)	As(2)-C(42)	2.00 (2)	As(2)-C(42)	1.94 (2)
C(31)-C(32)	1.531 (5)	C(41)-C(42)	1.33 (2)	As(1)-C(31)	1.92 (2)
		C(51)-C(52)	1.36 (3)	As(1)-C(32)	1.94 (1)
P(1)-C(41)	1.834 (4)	As(1)-C(31)	1.93 (2)	C(41)-C(42)	1.38 (2)
P(1)-C(51)	1.827 (3)	As(1)-C(32)	1.93 (2)	C(51)-C(52)	1.37 (2)
P(2)-C(61)	1.839 (4)	As(2)-C(51)	1.95 (2)	As(2)-C(33)	1.95 (2)
P(2)-C(71)	1.833 (3)	As(3)-C(52)	1.98 (2)	As(2)-C(51)	1.97 (2)
		As(2)-C(33)	1.95 (2)	As(3)-C(34)	1.93 (2)
		As(3)-C(34)	1.95 (2)	As(3)-C(35)	1.95 (2)
		As(3)-C(35)	1.94 (2)	As(3)-C(52)	1.96 (1)
Co(1)-C(11)	1.778 (4)	Co(1)-C(11)	1.74 (2)		
C(11)-O(11)	1.149 (4)	C(11)-O(11)	1.14 (2)	Co(2)-C(21)	1.77 (3)
Co(2)-C(21)	1.815 (4)	Co(2)-C(21)	1.80 (2)	C(21)-O(1)	1.12 (2)
C(21)-O(21)	1.134 (5)	C(21)-O(21)	1.12 (2)	Co(2)-C(22)	1.78 (3)
Co(2)-C(22)	1.810 (4)	Co(2)-C(22)	1.78 (3)	C(22)-O(2)	1.14 (2)
C(22)-O(22)	1.144 (4)	C(22)-O(22)	1.15 (2)	Co(2)-C(23)	1.79 (2)
Co(2)-C(23)	1.801 (3)	Co(2)-C(23)	1.81 (2)	C(23)-O(3)	1.15 (2)
C(23)-O(23)	1.138 (4)	C(23)-O(23)	1.13 (2)	Co(1)-C(23)	2.33 (2)
Bond Angles (deg)					
Co(2)-Co(1)-C(2)	50.9 (1)	Co(2)-Co(1)-C(2)	50.6 (6)	Co(2)-Co(1)-C(2)	50.8 (5)
Co(2)-Co(1)-C(3)	50.7 (1)	Co(2)-Co(1)-C(3)	49.9 (5)	Co(2)-Co(1)-C(3)	50.3 (5)
Co(1)-Co(2)-C(2)	49.5 (1)	Co(1)-Co(2)-C(2)	48.8 (6)	Co(1)-Co(2)-C(2)	50.2 (5)
Co(1)-Co(2)-C(3)	48.7 (1)	Co(1)-Co(2)-C(3)	49.8 (5)	Co(1)-Co(2)-C(3)	50.5 (5)
Co(1)-C(2)-Co(2)	79.6 (1)	Co(1)-C(2)-Co(2)	80.6 (7)	Co(1)-C(2)-Co(2)	78.9 (6)
Co(1)-C(2)-C(1)	149.3 (2)	Co(1)-C(2)-C(1)	144 (2)	Co(1)-C(2)-C(1)	140 (2)
Co(1)-C(2)-C(3)	68.1 (2)	Co(1)-C(2)-C(3)	70 (1)	Co(1)-C(2)-C(3)	69 (1)
Co(2)-C(2)-C(1)	126.4 (3)	Co(2)-C(2)-C(1)	129 (2)	Co(2)-C(2)-C(1)	134 (2)
Co(2)-C(2)-C(3)	69.3 (2)	Co(2)-C(2)-C(3)	69 (1)	Co(2)-C(2)-C(3)	69 (1)
Co(1)-C(3)-Co(2)	80.6 (1)	Co(1)-C(3)-Co(2)	80.3 (6)	Co(1)-C(3)-Co(2)	79.2 (7)
Co(1)-C(3)-C(2)	70.5 (2)	Co(1)-C(3)-C(2)	68 (1)	Co(1)-C(3)-C(2)	69 (1)
Co(1)-C(3)-C(4)	142.0 (3)	Co(1)-C(3)-C(4)	135 (1)	Co(1)-C(3)-C(4)	141 (1)
Co(2)-C(3)-C(2)	70.3 (2)	Co(2)-C(3)-C(2)	70 (1)	Co(2)-C(3)-C(2)	70 (1)
Co(2)-C(3)-C(4)	129.4 (2)	Co(2)-C(3)-C(4)	135 (2)	Co(2)-C(3)-C(4)	133 (1)
C(1)-C(2)-C(3)	132.1 (3)	C(1)-C(2)-C(3)	133 (2)	C(1)-C(2)-C(3)	134 (2)
C(2)-C(3)-C(4)	135.9 (3)	C(2)-C(3)-C(4)	138 (2)	C(2)-C(3)-C(4)	133 (2)
Co(2)-Co(1)-P(1)	157.4 (1)	Co(2)-Co(1)-As(1)	153.4 (1)	Co(2)-Co(1)-As(2)	150.0 (1)
Co(2)-Co(1)-P(2)	107.9 (1)	Co(2)-Co(1)-As(2)	112.0 (1)	Co(2)-Co(1)-As(1)	111.0 (1)
				Co(2)-Co(1)-As(3)	108.4 (1)
P(1)-Co(1)-P(2)	89.1 (1)	As(1)-Co(1)-As(2)	87.2 (1)	As(1)-Co(1)-As(2)	87.7 (1)
				As(1)-Co(1)-As(3)	106.3 (1)
				As(2)-Co(1)-As(3)	87.1 (1)
C(2)-Co(1)-P(1)	109.8 (1)	As(1)-Co(1)-C(2)	107.3 (5)	As(1)-Co(1)-C(2)	148.1 (5)
C(2)-Co(1)-P(2)	110.5 (1)	As(2)-Co(1)-C(2)	107.2 (6)	As(2)-Co(1)-C(2)	101.2 (5)
				As(3)-Co(1)-C(2)	104.7 (5)
C(3)-Co(1)-P(1)	107.7 (1)	As(1)-Co(1)-C(3)	104.2 (5)	As(1)-Co(1)-C(3)	107.6 (5)
C(3)-Co(1)-P(2)	150.5 (1)	As(2)-Co(1)-C(3)	148.1 (5)	As(2)-Co(1)-C(3)	102.6 (5)
				As(3)-Co(1)-C(3)	145.0 (5)
C(11)-Co(1)-P(1)	93.4 (1)	As(1)-Co(1)-C(11)	97.2 (6)		
C(11)-Co(1)-P(2)	99.4 (1)	As(2)-Co(1)-C(11)	100.4 (7)		
Co(1)-P(1)-C(31)	106.5 (1)	Co(1)-As(1)-C(41)	109.3 (5)	Co(1)-As(1)-C(41)	107.9 (5)
Co(1)-P(1)-C(41)	119.2 (1)	Co(1)-As(1)-C(31)	121.9 (8)	Co(1)-As(1)-C(31)	119.2 (6)
Co(1)-P(1)-C(51)	119.1 (1)	Co(1)-As(1)-C(32)	118.1 (6)	Co(1)-As(1)-C(32)	125.0 (5)
C(31)-P(1)-C(41)	102.0 (2)	C(41)-As(1)-C(31)	102.3 (8)	C(31)-As(1)-C(41)	102.1 (7)
C(31)-P(1)-C(51)	106.2 (1)	C(41)-As(1)-C(32)	101.8 (9)	C(32)-As(1)-C(41)	100.5 (7)
C(41)-P(1)-C(51)	102.0 (2)	C(31)-As(1)-C(32)	100.6 (9)	C(31)-As(1)-C(32)	98.6 (8)
Co(1)-P(2)-C(32)	107.3 (1)	Co(1)-As(2)-C(42)	107.1 (6)	Co(1)-As(2)-C(42)	109.1 (5)
Co(1)-P(2)-C(61)	123.1 (1)	Co(1)-As(2)-C(51)	122.2 (5)	Co(1)-As(2)-C(51)	109.7 (5)
Co(1)-P(2)-C(71)	115.3 (1)	Co(1)-As(2)-C(33)	119.1 (6)	Co(1)-As(2)-C(33)	127.5 (5)
C(32)-P(2)-C(61)	100.3 (2)	C(42)-As(2)-C(51)	103.6 (8)	C(33)-As(2)-C(42)	101.2 (7)
C(32)-P(2)-C(71)	106.5 (1)	C(42)-As(2)-C(33)	100.7 (8)	C(33)-As(2)-C(51)	102.5 (7)
C(61)-P(2)-C(71)	102.4 (2)	C(51)-As(2)-C(33)	101.3 (8)	C(42)-As(2)-C(51)	104.6 (6)

Table IV (Continued)

5		7		8 ^a	
		C(34)-As(3)-C(35)	98 (1)	C(34)-As(3)-C(35)	98.7 (8)
		C(52)-As(3)-C(34)	99 (1)	C(34)-As(3)-C(52)	102.9 (8)
		C(52)-As(3)-C(35)	98 (1)	C(35)-As(3)-C(52)	103.7 (7)
		As(1)-C(41)-C(42)	117 (1)	Co(1)-As(3)-C(52)	107.5 (5)
		As(2)-C(42)-C(41)	118 (1)	Co(1)-As(3)-C(34)	124.7 (6)
				Co(1)-As(3)-C(35)	116.9 (5)
P(1)-C(31)-C(32)	111.4 (2)			As(1)-C(41)-C(42)	118 (1)
P(2)-C(32)-C(31)	111.2 (2)			As(2)-C(42)-C(41)	116 (1)
Co(2)-Co(1)-C(11)	98.1 (1)	Co(2)-Co(1)-C(11)	97.2 (6)		
C(2)-Co(1)-C(11)	141.7 (1)	C(11)-Co(1)-C(2)	143.6 (9)		
C(3)-Co(1)-C(11)	103.4 (1)	C(11)-Co(1)-C(3)	107.4 (8)		
Co(1)-C(11)-O(11)	175.9 (3)	Co(1)-C(11)-O(11)	171 (2)		
Co(1)-Co(2)-C(21)	103.2 (1)	Co(1)-Co(2)-C(21)	96.2 (6)	Co(1)-Co(2)-C(21)	126.6 (8)
C(2)-Co(2)-C(21)	100.0 (1)	C(21)-Co(2)-C(2)	103.4 (8)	C(2)-Co(2)-C(21)	132 (1)
C(3)-Co(2)-C(21)	139.4 (1)	C(21)-Co(2)-C(3)	140.1 (8)	C(3)-Co(2)-C(21)	96 (1)
Co(2)-C(21)-O(21)	176.5 (3)	Co(2)-C(21)-O(21)	178 (2)	Co(2)C(21)-O(1)	177 (3)
Co(1)-Co(2)-C(22)	96.1 (1)	Co(1)-Co(2)-C(22)	99.5 (7)	Co(1)-Co(2)-C(22)	126.9 (7)
C(2)-Co(2)-C(22)	141.0 (2)	C(22)-Co(2)-C(2)	137.9 (8)	C(2)-Co(2)-C(22)	98.4 (8)
C(3)-Co(2)-C(22)	105.4 (2)	C(22)-Co(2)-C(3)	99.3 (8)	C(3)-Co(2)-C(22)	134.2 (8)
Co(2)-C(22)-O(22)	179.2 (3)	Co(2)-C(22)-O(22)	178 (2)	Co(2)-C(22)-O(2)	177 (2)
Co(1)-Co(2)-C(23)	148.5 (1)	Co(1)-Co(2)-C(23)	150.1 (7)	Co(1)-Co(2)-C(23)	64.5 (6)
C(2)-Co(2)-C(23)	105.5 (1)	C(23)-Co(2)-C(2)	103.4 (9)	C(2)-Co(2)-C(23)	110.5 (8)
C(3)-Co(2)-C(23)	100.1 (1)	C(23)-Co(2)-C(3)	103.1 (8)	C(3)-Co(2)-C(23)	110.1 (8)
				Co(2)-Co(1)-C(23)	43.7 (5)
				Co(1)-C(23)-O(3)	127 (2)
				Co(1)-C(23)-Co(2)	71.8 (7)
Co(2)-C(23)-O(23)	177.7 (3)	Co(2)-C(23)-O(23)	173 (2)	Co(2)-C(23)-O(3)	160 (2)
C(21)-Co(2)-C(22)	106.5 (2)	C(21)-Co(2)-C(22)	107.5 (9)	C(21)-Co(2)-C(22)	106 (1)
C(21)-Co(2)-C(23)	99.8 (2)	C(21)-Co(2)-C(23)	102.1 (9)	C(21)-Co(2)-C(23)	102 (1)
C(22)-Co(2)-C(23)	97.7 (1)	C(22)-Co(2)-C(23)	97 (1)	C(22)-Co(2)-C(23)	102.7 (8)

^aData from ref 4.Table V. NMR Spectra 2-8^a

compd	³¹ P{ ¹ H} ^b	¹⁹ F ^{c,e}	¹ H ^d	¹³ C{ ¹ H} ^d
2	39.1 (d) -27.8 (d, ² J _{PP} = 65.5 Hz)	-46.4 (s)	7.25-7.16 (m, 20 H) 3.07 (dd, J _{P-H} ≈ 8.1 Hz, J _{H-H} = 1 Hz, 2 H)	134-126 (m, 24 C) 31.6, 30.6 (J _{P-C} = 1.79, J _{P-C} = 0.97, CH ₂)
3'	37.0 (s) 7.7 (s)			
3	37.7 (s)	-46.2 (t, ² J _{P-F} = 4.7 Hz) -44.3 (s), -48.1 (s)	7.25 (m, 20 H) 3.34 (t, ² J _{P-H} = 10.8 Hz, 2 H)	201.2 (CO), 136-128 (m, 24 C) 37.9 (t, ² J _{P-H} = 7.9 Hz, 2 C)
4	41.9 (s, 2 P)	-45.9 (s, 12 F)	7.5 (m, 20 H) 2.20 (t, 4 H)	197.6 (CO), 133-128 (m, 24 C)
5	66.7 (s) 37.0 (br, w) 67.9 (s)	-43.5 (s, 6, F)	7.35 (m, 20 H) 2.60 (t, ² J _{P-H} ≈ 1 Hz, 2 H) 2.43 (t, ² J _{P-H} ≈ 1 Hz, 2 H)	199.1 (CO)8 133-128 (m, 24 C) 32.2 (s, 4 C), 20.0 (s, 1 C)
7	...	-46.5 (s, br) -45.2 (s, br)	7.85-7.35 (m, 8 H) 1.85, 1.70, 1.60 (s, CH ₃ on bound As, each 3 H) 1.02, 0.43 (s, CH ₃ on dangling As, each 3 H)	200.0 (CO) 146.7-129.1 (C ₆ H ₄ , 12 C) 135.1, 123.3 (CF ₃) 16.1, 14.2 (s, CH ₃) 11.3, 10.6 (s, CH ₃)
8	...	-43.1 (s, sh)	7.9-7.4 (m, 8 H) 1.94 (s, endo) 1.65 (s, exo) 1.41 (s, central CH ₃ , 6 H)	212.4 (CO) 142.8, 12.8 (C ₆ H ₄) 128.3 (q, ² J _{C-F} = 268 Hz, CF ₃) 13.9 (terminal CH ₃ , 6 H) 11.5 (central, CH ₃ , 3 H)

^appm in CDCl₃ at 293 K unless data in italics when the temperature is 233 K. The ³¹P and ¹⁹F spectra of 2, 3, and 5-8 are critically dependent on the temperature at which the spectra are recorded. This is discussed in detail elsewhere. Abbreviations: s, singlet; d, doublet; m, multiplet; br, broad; sh, sharp. ^b85% H₃PO₄ external standard. ^cCFCl₃ external standard. ^dMe₄Si internal standard. ^eFor comparison [μ -(CF₃)₂C₂]Co₂(CO)₆¹⁹F NMR δ -53.0. ^fIn CD₂Cl₂.

significance to the discussion here. The angles subtended at Co(1) by the two arsenic donor atoms in 7, 87.2°, are similar to the corresponding angles in 8 although the angle subtended by the terminal arsenic atoms, As(1) and As(3), in this compound, 106.3°, is large by comparison. This can be attributed to the close contacts between the methyl group hydrogens that result if the ligand is constrained to occupy three facial sites in octahedral coordination.

Structures of 2-8. NMR data are given in Table V. Analysis of 2 suggests a η^1 rather than a μ - η^1 structure, and this is confirmed by the spectroscopic data. A criterion for the extent of ligation is the energy of the A₁ ν (CO)_{sym}

mode, and an energy of 2092 cm⁻¹ for 2 is consistent with a η^1 -dppm coordination. The ¹H NMR spectrum at 293 K has an ABXY pattern with J_{H_AH_B} = 8 Hz and J_{PCH₂} ≈ 1 Hz. At 233 K the ³¹P{¹H} NMR spectrum showed resonances at δ 39.1 and -27.8 (J(PP¹) = 64.5 Hz), which can be assigned to the coordinated and "dangling" phosphorus atoms, respectively;²⁹ the uncoordinated resonance is sharp whereas the coordinated (39.1 ppm) is broad at 233 K but sharp at 293 K as a result of the quadrupole broadening

by ^{59}Co . The ^{19}F resonance is a singlet at all temperatures. The structure of **6** is assigned as η^1 from the similarity of its infrared spectrum with that of **2**.

Spectroscopic data are consistent with a μ - η^2 configuration for **3** in all solvents. The $^{31}\text{P}\{^1\text{H}\}$ NMR spectrum shows that the phosphorus atoms are chemically equivalent while a triplet is seen in the methylene region in the $^1\text{H}\{^{31}\text{P}\}$ NMR spectrum at 293 K ($J_{\text{P-H}} = 11.2$ Hz); the expected ABX₂ pattern for the methylene is not resolved at 213 K. Stereochemical nonrigidity, which is a feature of these μ -alkyne complexes, is manifested in the temperature-dependent ^{19}F NMR spectra of **3** in CH_2Cl_2 . A time-averaged spectrum ($\delta -46.2$ (t, $J_{\text{CF}_3\text{P}} = 4.7$ Hz), at 323 K collapses to a static spectrum at 233 K ($\delta -47.8$ and -44.6). An analysis of this nonrigidity, and that of the other derivatives, will be presented in detail elsewhere, but these data fully support the alkyne-rocking motion suggested by Hansen and Mancini³⁰ in which the motion generates a mirror plane containing the two P atoms and the two Co atoms.

Formulation of **3'** rests on the spectroscopic data. The energy of the A₁ mode shows that both phosphorus atoms are coordinated to one $\text{Co}_2(\text{CO})_6$ unit and the $\nu(\text{CO})$ profile is similar to that of **5**. Two broad $^{31}\text{P}\{^1\text{H}\}$ resonances at 233 K show that the phosphorus atoms are nonequivalent on the NMR time scale as expected for a η^2 -dppm structure. The lability of **3'** precluded measurement over a wide temperature range.

The initial dppe complex **4** has a binuclear μ - η^1 configuration in solution shown by (i) the A₁ mode at 2092 cm^{-1} , (ii) the sharp singlet in the $^{31}\text{P}\{^1\text{H}\}$ NMR spectrum at 233 K, (iii) a singlet $^{19}\text{F}(\text{CF}_3)$ resonance, (iv) the pattern in the methylene region of the $^1\text{H}\{^{31}\text{P}\}$ NMR spectrum, and (v) a methylene triplet in the $^{13}\text{C}\{^1\text{H}\}$ NMR spectrum.

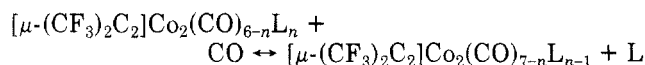
A η^2 pseudoaxial-pseudoequatorial conformation for **5** is consistent with the nonequivalent CH_2 groups in the $^1\text{H}\{^{31}\text{P}\}$ NMR and $^{13}\text{C}\{^1\text{H}\}$ NMR spectra at 298 K and the $\nu(\text{CO})$ spectrum which is different to that of a μ - η^2 complex (cf. **3**) but similar to the KBr $\nu(\text{CO})$ spectrum of crystalline **7**. The static η^2 structure generates nonequivalent CF_3 and $\text{P}(\text{CH}_2)$ groups, but this was not shown by the ^{19}F or ^{31}P spectra in the temperature range 298–233 K presumably because of the alkyne-rocking motion alluded to above. We note that the activation energy is lower in the dppe relative to the dppm complexes.

The solution spectra of **7** are consistent with the crystal structure. As long as there is no free rotation about the central As–C bond of ttas, the lowest energy conformation (minimum steric strain) is one in which the terminal CH_3 groups are stereochemically nonequivalent—consequently in ttas itself three CH_3 resonances are observed. This nonequivalence is retained in **7** and results in five resonances, those at 0.43 and 1.02 ppm being assigned to the “dangling” Me_2As group. The number of CH_3 and phenyl resonances in the $^{13}\text{C}\{^1\text{H}\}$ spectrum argues against a symmetrically bound ttas and is consistent with an pseudoaxial-equatorial chelate conformation. As noted above this chelate conformation generates nonequivalent CF_3 groups on the alkyne in the static structure and this is seen in the ^{19}F spectrum where two broad singlets are seen at 233 K. Nonetheless, the temperature dependence of the ^{19}F spectrum show that the stereochemical nonrigidity is more complex than anticipated as at 273 K another pair of singlets is observed which do not apparently collapse to a time-averaged resonance. We analyze this behavior elsewhere but note that the static structure is clearly not

retained in solution at ambient temperature.

Analysis of the spectroscopic data for the thermodynamically stable ttas complex **8** reveals that there is a structural change from the static structure upon dissolution in organic solvents. In KBr a weak $\nu(\text{CO})$ band at 1865 cm^{-1} can be assigned to the semibridging carbonyl group, but this band is absent in all solution spectra. Furthermore, the solution spectra show four or five terminal $\nu(\text{CO})$ bands, the relative intensities of which are markedly affected by the polarity of the solvent. From the solvent effect we can recognize two sets of $\nu(\text{CO})$ bands, one set at 2054, 2001, and 1979 cm^{-1} and the other at 2044, 2035, and 1990 cm^{-1} , and a comparison with the KBr spectra allows an assignment of the first set to the static structure **8**.

^{13}CO Substitution of **1 by ETC Methods.** A high degree of ^{13}CO substitution was desirable for some of the derivatives in order to record temperature-dependent ^{13}C NMR. The usual method of ^{13}CO substitution is slow for $[\mu-(\text{CF}_3)_2\text{C}_2]\text{Co}_2(\text{CO})_{6-n}\text{L}_n$ derivatives, but recognizing that CO can be a nucleophile in an ETC cycle we utilized a BPK-initiated cycle to achieve up to 25% substitution with **1** (higher percentages could be achieved, see Experimental Section). This method is much faster and more convenient than traditional methods and can be utilized even when the formal ETC cycle is not particularly efficient. Direct substitution of the Lewis base derivatives is possible, but losses occur through the equilibrium ($n \neq 0$).



Conclusion

This work has demonstrated that selective ligation of the $(\mu\text{-alkyne})\text{Co}_2(\text{CO})_x$ moiety can be achieved by using electrocatalytic methods. Current interest in transition-metal clusters arises in part from their potential as homogeneous catalysts. Catalytic activity requires coordinative unsaturation, but often a compromise has to be reached between instability induced by coordinative unsaturation and reactivity. When stability is maintained with bridging polydentate ligands, one often reduces the activity. Selective ETC catalyzed substitution offers an alternative means of achieving both objectives since, providing the homogeneous reactions with the reactants (e.g. CO/H_2) are fast, coordinative unsaturation is inherently generated by the electrocatalytic process. Substitution of the CO groups is very fast by these techniques with the catalytic efficiency decreasing as the extent of substitution increases.

The selectivity and rates of electrocatalytic reactions are much better with $[\mu-(\text{CF}_3)_2\text{C}_2]\text{Co}_2(\text{CO})_6$ as the substrate than in the other system investigated in detail, the tricobalt-carbon cluster $\text{RCCO}_3(\text{CO})_9$.^{5,9} As the lifetime of the radical anions $[\mu-(\text{CF}_3)_2\text{C}_2]\text{Co}_2(\text{CO})_6^-$ and $\text{RCCO}_3(\text{CO})_9^-$ are similar, the advantages of the former substrate must lie in the relative rates of nucleophilic attack, ring closure, and homogeneous electron transfer and, possibly, the lability of the coordinated ligand. Since these factors are important in utilizing selective ETC substitution to generate partially ligated molecules for catalytic purposes, we investigated the redox chemistry of the products by electrochemical methods—this work is described in the following paper.¹⁰

Acknowledgment. We thank the Chemistry Department, University of Waikato, for their hospitality and use of NMR facilities and Dr. W. T. Robinson, University of Canterbury, for the x-ray data collection.

Registry No. 1, 37685-63-5; 2, 108151-11-7; 3, 84896-13-9; 3', 108151-17-3; 4, 108151-12-8; 5, 108151-13-9; 5', 108151-14-0; 6, 87828-96-4; 7, 87828-97-5; 8, 87828-98-6; BPK, 16592-08-8; dppm, 2071-20-7; dppe, 1663-45-2; ttas, 2774-08-5.

Supplementary Material Available: Thermal parameters of non-hydrogen atoms (Tables S3 and S4), positional parameters

for calculated hydrogen atoms (Tables S5 and S6), additional bond length and angle data (Tables S7 and S8), and selected least-squares planes (Tables S9 and S10), and selected intra- and intermolecular nonbonded contacts (Table S11) for 5 and 7 (12 pages); listings of structure factors for 5 and 7 (Tables S1 and S2) (31 pages). Ordering information is given on any current masthead page.

Electron Transfer in Organometallic Clusters. 13. Catalytic Sequential Ligation of $[\mu-(\text{CF}_3)_2\text{C}_2]\text{Co}_2(\text{CO})_6$ by Polydentate Ligands and Electrochemistry of Derivatives

Simon D. Jensen, Brian H. Robinson,* and Jim Simpson*

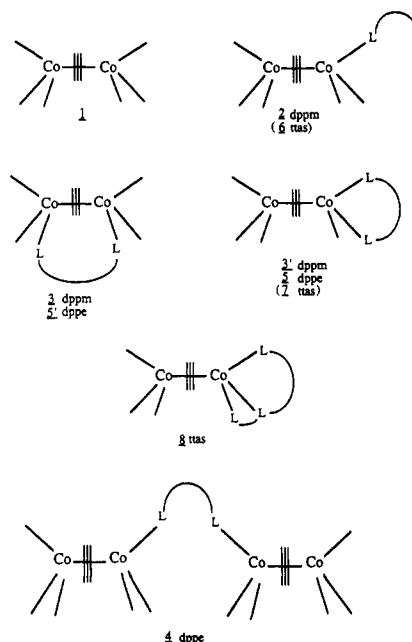
Department of Chemistry, University of Otago, P.O. Box 56, Dunedin, New Zealand

Received December 4, 1986

Analysis of i - E responses for $[\mu-(\text{CF}_3)_2\text{C}_2]\text{Co}_2(\text{CO})_{6-n}(\text{L-L})$ (L-L = dpmm, dppe, ttas), $\{[\mu-(\text{CF}_3)_2\text{C}_2]\text{Co}_2(\text{CO})_{5/2}(\text{dppe})\}$, and $[\mu-\text{Ph}_2\text{C}_2]\text{Co}_2(\text{CO})_4(\text{L-L})$ (L-L = dpmm, dppe) provides an understanding of the electron transfer catalyzed sequential substitution of $[\mu-(\text{CF}_3)_2\text{C}_2]\text{Co}_2(\text{CO})_6$ by polydentate ligands. All derivatives undergo a primary one-electron reduction step at the cluster center which is electrochemically and chemically reversible when $n = 2$ but chemically irreversible for $n = 1$ due to subsequent ETC reactions and rapid structural rearrangements. Electron transfer to the μ - η^1 -dppe complex cleaves the dppe bridge to give a η^1 -radical anion and $[\mu-(\text{CF}_3)_2\text{C}_2]\text{Co}_2(\text{CO})_5^-$ while an axial-equatorial rearrangement occurs when the η^1 -dpmm complex is reduced. The ttas derivatives, $n = 2$ and 3, undergo reversible one-electron oxidation at the ligand, and oxidation of the cluster also occurs for $n = 3$. Homogeneous electron transfer chain (ETC) catalyzed sequential substitution occurs with decreasing catalytic efficiency as n increases; for L-L = ttas the transformation $n = 2 \rightarrow n = 3$ is not catalyzed. Fast structural rearrangements are observed during catalysis, and the primary substitution rate is in the order ttas > dppe > dpmm, but the ring closure rate is in the order ttas > dpmm > dppe.

An understanding of how a metal carbonyl cluster responds structurally in an electron transfer reaction is important to the design of electrocatalytic cluster systems and to stereospecific syntheses involving electron transfer. Questions such as whether structural change occurs before or after the homogeneous electron transfer step are central to a determination of rates of heterogeneous and homogeneous transfer and to the rate of nucleophilic or electrophilic attack at the reduced or oxidized center.² If we restrict discussion to a reductive electron transfer, the dominant redox behavior with carbonyl cluster compounds,³ the structural changes which can occur range from changes in molecular parameters like metal-metal bond lengths (in which case electron transfer is usually fast^{2,4}), through isomerization,^{5,6} to completely different bond connectivities⁷ and/or ligand dissociation.^{5,8} From an electrochemical view these structural changes influence the height of the activation barrier between reactant and

Scheme I^a



^a ≡ corresponds to the acetylene ligand $(\text{CF}_3)_2\text{C}_2$.

(1) Part 12: *Organometallics* preceding paper in this issue.

(2) Geiger, W. E. *Prog. Inorg. Chem.* **1985**, *33*, 275.

(3) Lemoine, P. *Coord. Chem. Rev.* **1982**, *47*, 55.

(4) Maj, J. J.; Rae, A. D.; Dahl, L. F. *J. Am. Chem. Soc.* **1982**, *104*, 3054.

(5) Downard, A. J.; Robinson, B. H.; Simpson, J. *Organometallics* **1986**, *5*, 1122. Downard, A. J.; Robinson, B. H.; Simpson, J. *Organometallics* **1986**, *5*, 1140.

(6) Arewgoda, C. M.; Robinson, B. H.; Simpson, J. *J. Chem. Soc., Chem. Commun.* **1982**, 284.

(7) Cyr, J. E.; De Gray, J. A.; Gosser, D. K.; Lee, E. S.; Rieger, P. H. *Organometallics* **1985**, *4*, 950. Bond, A. M., Downard, A. J.; Robinson, B. H.; Simpson, J. *J. Organomet. Chem.*, in press.

(8) Bond, A. M.; Dawson, P. A.; Peake, B. M.; Robinson, B. H.; Simpson, J. *Inorg. Chem.* **1977**, *16*, 2199.

product and, consequently, the electrochemical reversibility.

A variety of ligational modes are often possible for carbonyl cluster polydentate Lewis base derivatives, and this can make the quantitative interpretation of the